Forward electroproduction of pion beyond resonances in the Reggeized model

Byung Geel Yu,[1,*] Tae Keun Choi,[2] and Kook Jin Kong[1]

[1] *Research Institute of Basic Sciences, Korea Aerospace University, Koyang 412-791, Korea*

[2] *Department of Physics, Yonsei University, Wonju 412-791, Korea*

(Dated: December 18, 2024)

We present an analysis of exclusive electroproduction of pions in both charged $N(e,e'\pi^{\pm})N$ and neutral $N(e,e'\pi^0)N$ channels within the framework of the Reggeized model. In this model, we consider the exchange of mesons in the t-channel, including $\pi(140)$, $b_1(1235)$, $\rho(775)$, $a_2(1320)$ and $a_1(1260)$ for charged processes, and $\omega(782)$, $\rho^0(775)$, $h_1(1170)$ and $b_1(1235)$ for neutral processes. We investigate the dependence of electroproduction cross sections on the squared four-momentum transfer $-t$ and the negative of the squared four-momentum transferred by the electron Q^2, utilizing experimental data from DESY, CEA, and recent data from JLAB. This analysis provides insights into the underlying dynamics of pion electroproduction and contributes to our understanding of hadronic interactions at high energies.

PACS numbers: 13.60.Le, 13.60.-r, 13.60.Rj

I. INTRODUCTION

Electroproduction of pion is a useful tool for studying hadron phenomenology using electromagnetic probes. At low energies, it provides information on the dynamic properties of Δ and N^* resonances as well as quantitative properties of the πN system [? ?]. At high energies beyond the resonances, the reaction mechanism is well described by the exchange of mesons at forward angles. The Regge model is valid for such purposes and has been widely applied to a number of hadron reactions involving meson exchange in the t-channel [? ?]. In charged reactions the role of pion exchange is conspicuous due to its large coupling constant $g_{\pi NN}$, while the electric Born term of the nucleon is considered to preserve gauge invariance of the pion exchange. In the neutral channel, as the absence of pion exchange due to the conservation of charge conjugation, the reaction is accounted for by the exchange of neutral vector and axial vector mesons [? ?].

To date, both experimental and theoretical analyses of pion electroproduction have shown that the longitudinal cross section is primarily determined by the dominance of the pion pole, specifically through the pion charge form factor $F_\pi(Q^2)$. On the other hand, the transverse cross section is described by the nucleon pole, primarily through the nucleon charge form factor $F_1(Q^2)$. Therefore, the role of these components is stressed in understanding the production mechanism of the reaction, and hence, extracting the pion form factor from experimental data has been one of significant topics in both sides of theory and experiment [? ? ?].

Meanwhile, in model calculations, that the nucleon pole is assumed to be on-mass shell may leads to the underestimation of the transverse cross section with the use of the on-shell cutoff mass for the nucleon charge form factor. Therefore, it is a significant challenge to resolve the discrepancy between experimental and theoretical predictions regarding the transverse cross section in the reaction [? ? ? ?].

On the other hand, it is expected that the high virtuality Q^2 of virtual photon in electroproduction offers a chance to investigate the distribution of partons in the deep structure of hadrons [? ? ?]. Recently, there has been plans to apply pion electroproduction to nuclei in future accelerators such as the Electron-Ion Collider (EIC) to identify QCD evidence in nuclei. It is therefore desirable to establish a theory for pion electroproduction that covers the range of energy, angle, and virtuality encompassed in the current world data.

In this paper we investigate pion electroproduction in four channels, $\gamma^* N \to \pi^{\pm} N$ and $\gamma^* N \to \pi^0 N$, based on our previous work [?] on the photoproduction case. Thus, the simple model consisting of pion and rho-meson exchange is extended to incorporate the exchange of tensor meson and axial vector meson, which were previously disregarded due to the exchange degeneracy. The reactions at proton and neutron targets in charged as well as neutral processes are bounded by the isospin symmetry where the phase of the Regge trajectories between meson exchanges will be chosen the same as in photoproduction [?]. Given the same set of coupling constants and Regge trajectories for electroproduction as well, only the electromagnetic form factor of hadrons are further introduced to the production amplitudes involved in the virtual photon coupling. Such an extended version in the real photon case [?] enables us to reduce the coupling constants of vector mesons to more moderate values, because of the same trajectory with the ρ meson. Furthermore, the inclusion of these mesons of high spin and large mass yields an improvement of model predictions for spin polarization observables.

This paper is organized as follows. In Sec. II, we provide a brief overview of the kinematics and definitions of cross sections in the exclusive electroproduction reaction. We discuss our treatment of gauge-invariant

* bgyu@kau.ac.kr

pion exchange based on the Gross-Riska prescription [?]. The Regeeized model is presented, followed by a discussion in Sec. IV concerning the inclusion of high spin meson exchanges with form factors coupling to virtual photon. An examination of the exclusive-inclusive relationship follows in Section V, where we analyze the role of the vector $\rho(775)$ and tensor meson $a_2(1270)$, axial vector meson $a_1(1260)$ and $b_1(1235)$ for charged, and $h_1(1117)$ Regge trajectories for neutral processes. In Section VI, we provide a brief discussion of $\pi^{\pm}$ photoproduction at forward angles. The model is presented thereafter. Extended to electroproduction, the results are compared to experimental data from JLAB, DESY, and Cornell in Sections VII?IX. In Section X, a comparison is made between our results and those from the HERMES data. Section XI proceeds to analyze the Q^2 behavior of the cross sections. The discussion of the polarized beam-spin asymmetry and the role of axial vector and tensor mesons in $(e, e\pi^{\pm})$ can be found in Section XII. In Section 13, this paper presents the model predictions for JLAB at 12 GeV. The summarized conclusions are available in Section 14. Some of the calculation details have been moved to the Appendices.

II. ELECTROPRODUCTION OF PSEUDOSCALAR MESON

We briefly introduce the kinematics in the exclusive π electroproduction,

$$e(\kappa) + N(p) \to e(\kappa) + N(p') + \pi(q), \tag{1}$$

and denote the notations and definitions of variables. The mandelstam variables for the reaction in the three channel are

$$\begin{aligned} s &= (p+k)^2 = (p'+q)^2, \\ t &= (q-k)^2 = (p-p')^2, \\ u &= (p-q)^2 = (p'-k)^2 \end{aligned} \tag{2}$$

with the virtual photon momentum $k^2 = \kappa'^2 - \kappa^2$ in terms of the initial and the final electron momenta κ and κ'. The virtuality of photon is given by $Q^2 = -k^2$.

In the electroproduction fully expressed in Eq. (1) where the target nucleon is at rest, the z-axis is directed along the three momentum of the virtual photon γ^* which is defined as $\vec{k} = \left(0,\, 0,\, \sqrt{\nu^2+Q^2}\right)$ with the virtual photon four-momentum $k = \kappa - \kappa' = \left(\nu,\, \vec{k}\right)$, $\nu = E_e - E'_e$ in the laboratory system.

More variables are the Bjorken scaling variable $x_B = Q^2/2M\nu$ as the fraction of the target nucleons momentum carried by the struck quark, and the invariant energy in the γ^*-N system, $W^2 = M^2 + 2M\nu - Q^2 = M^2 + Q^2\left(\frac{1}{x_B} - 1\right)$.

The S-matrix element for electroproduction is[1]

$$S = \frac{1}{(2\pi)^{7/2}} \frac{m_e\sqrt{MM'}}{\sqrt{2E_\gamma q_0 E_e E'_e E E'}} i\delta^4(p+k-p'-q)\mathcal{M}_{fi} \tag{3}$$

$$\frac{d^3\sigma}{dE'_e d\Omega'_e d\Omega_\pi} = \Gamma \frac{d\sigma}{d\Omega_\pi} \tag{4}$$

where the flux of the electron current is given by

$$\Gamma = \frac{\alpha}{2\pi^2}\frac{E'_e}{E_e}\frac{K_H}{Q^2}\frac{1}{1-\epsilon}, \tag{5}$$

with the equivalent photon lab-energy $K_H = \frac{W^2-M^2}{2M}$. Electron polarization $\epsilon = \left[1 + 2\frac{\nu^2+Q^2}{4E_e(E_e-\nu)-Q^2}\right]^{-1}$ is the ratio of the longitudinal to the transverse polarization of the virtual photon, which is rewritten as $\epsilon = \frac{1-y-\frac{Q^2}{4E_e^2}}{1-y+\frac{y^2}{2}+\frac{Q^2}{4E_e^2}}$ in terms of $y = \nu/E_e$. The longitudinal component $\epsilon_L = \left(Q^2/\nu^2\right)\epsilon$. In terms of electron scattering angle, the electron polarization $\epsilon = \left(1 + \frac{2|\vec{k}|^2}{Q^2}\tan\frac{1}{2}\theta_e\right)^{-1}$ measured by the angle θ_e deviated from the reaction plane.

Separating the kinematical part of electron scattering in Eq. (3) the full cross section for virtual photoproduction

$$\gamma^*(k) + N(p) \to N(p') + \pi(q) \tag{6}$$

is expressed as follows[2],

$$\begin{aligned} \frac{d\sigma_{\rm tot}}{d\Omega_\pi} &= \frac{d\sigma_U}{d\Omega_\pi} + \epsilon\frac{d\sigma_{TT}}{d\Omega_\pi}\cos 2\Phi_\pi \\ &\quad + \sqrt{2\epsilon(\epsilon+1)}\,\frac{d\sigma_{TL}}{d\Omega_\pi}\cos\Phi_\pi, \end{aligned} \tag{7}$$

where the unpolarized cross section is given by

$$\frac{d\sigma_U}{d\Omega_\pi} = \frac{d\sigma_T}{d\Omega_\pi} + \epsilon\frac{d\sigma_L}{d\Omega_\pi}, \tag{8}$$

and $\frac{d\sigma_T}{d\Omega_\pi}$, $\frac{d\sigma_L}{d\Omega_\pi}$, $\frac{d\sigma_{TT}}{d\Omega_\pi}$, and $\frac{d\sigma_{LT}}{d\Omega_\pi}$ are the transverse, longitudinal, transverse-transverse, and longitudinal-transverse cross sections, respectively.

---

[1] For photoproduction the S-matrix element is given by

$$S = \frac{1}{(2\pi)^2}\sqrt{\frac{MM'}{4E_\gamma q_0 E E'}}\, i\delta^4(p+k-p'-q)\mathcal{M}_{fi}$$

[2] Note that the CEA [?] and the Cornell experiments [? ?] follow the convention for the polarization factor $d\sigma_{LT}$ cross section in Eq. (7),

$$\sqrt{\epsilon(\epsilon+1)/2}\,\frac{d\sigma_{TL}}{d\Omega_\pi}\cos\Phi_\pi.$$

III. THE REGGEIZED MODEL

For completeness we consider in this work the reaction proceeding via four channels as below.

$$\gamma^* p \to \pi^+ n\,, \tag{9}$$
$$\gamma^* n \to \pi^- p\,, \tag{10}$$
$$\gamma^* p \to \pi^0 p\,, \tag{11}$$
$$\gamma^* n \to \pi^0 n\,, \tag{12}$$

A. Electroproduction amplitudes

We utilize the effective Lagrangians for the construction of the Born approximation amplitude to one-photon exchange at the tree level. It is, then, extended to reggeize the meson exchange in the t-channel, following the prescription in Ref. [**?** **?**].

For the charged pion process, the charge conjugation C-even exchange in the t channel is allowed with the sign of the photon-meson coupling constant determined from the G-parity counting. Thus, the G-parity-even exchanges $\pi^\pm$, $a_1^\pm$, and $a_1^\pm$ have the opposite signs when coupling to photon between π^+ and π^- reactions. However, in order to avoid confusion caused by the signs of the coupling constants when considering the phase of the Regge propagators between exchange-degenerate pair $\{\rho - a_2\}$, for instance, we will write the signs in absolute values in $g_{\gamma\pi a_1}$ and $g_{\gamma\pi a_2}$, with the sign-opposite only appearing in the pion exchanges in the production amplitudes below. The signs of a_1 and a_2 coupling constants will then be included in the amplitudes in Eqs. (20) and (**??**) later, which are the final expressions containing the phases desired for the current calculation.

Therefore, the reggeized amplitudes for charged pion electroproduction are written as [**?**],

$$\mathcal{M}_{\pi^+ n} = i\sqrt{2}\, e g_{\pi NN}\bar{u}'(p')\left[\widetilde{F}_\pi(Q^2)\frac{(2q-k)\cdot\epsilon}{t-m_\pi^2}\gamma_5 + \gamma_5\frac{(\not{p}+\not{k}+M_p)}{s-M_p^2}\Gamma_{\gamma^* NN}(Q^2)\right]u(p)(t-m_\pi^2)\mathcal{R}^\pi(s,t)\,, \tag{13}$$

$$\mathcal{M}_{\pi^- p} = -i\sqrt{2}\, e g_{\pi NN}\bar{u}'(p')\left[\widetilde{F}_\pi(Q^2)\frac{(2q-k)\cdot\epsilon}{t-m_\pi^2}\gamma_5 - \Gamma_{\gamma^* NN}(Q^2)\frac{(\not{p}-\not{q}+M_p)}{u-M_p^2}\gamma_5\right]u(p)(t-m_\pi^2)\mathcal{R}^\pi(s,t)\,, \tag{14}$$

$$\mathcal{M}_V = \frac{g_{\gamma\pi V}}{m_0}F^\rho(Q^2)\varepsilon_{\mu\nu\alpha\beta}\epsilon^\mu k^\nu q'^\alpha(-g^{\beta\rho} + q'^\beta q'^\rho/m_V^2)\bar{u}'(p')\left[g^v_{VNN}\,\gamma_\rho + i\frac{g^t_{VNN}}{2M}\sigma_{\lambda\rho}q'^\lambda\right]u(p)\mathcal{R}^V(s,t)\,, \tag{15}$$

$$\mathcal{M}_T = \frac{2g_{\gamma\pi T}}{m_0^2}\,F^T(Q^2)\varepsilon_{\mu\nu\alpha\beta}\,\epsilon^\mu\,k^\nu q'^\alpha q_\rho\Pi^{\beta\rho;\lambda\sigma}(q-k)\bar{u}'(p')\left[\frac{2g^{(1)}}{M}(\gamma_\lambda P_\sigma + \gamma_\sigma P_\lambda) + \frac{4g^{(2)}}{M^2}P_\lambda P_\sigma\right]u(p)\mathcal{R}^T(s,t) \tag{16}$$

$$\mathcal{M}_A = i\frac{g_{\gamma\pi A}}{m_0}F^A(Q^2)(k\cdot q'\,\epsilon_\mu - \epsilon\cdot q'\,k_\mu)(-g^{\mu\nu} + q'^\mu q'^\nu/m_A^2)g^v_{ANN}\,\bar{u}'(p')\gamma_\nu\gamma_5 u(p)\mathcal{R}^A(s,t)\,, \tag{17}$$

$$\mathcal{M}_B = i\frac{g_{\gamma\pi B}}{m_0}F^B(Q^2)(k\cdot q'\,\epsilon_\mu - \epsilon\cdot q'\,k_\mu)(-g^{\mu\nu} + q'^\mu q'^\nu/m_B^2)\bar{u}'(p')i\frac{g^t_{BNN}}{2M}\sigma_{\lambda\nu}q'^\lambda\gamma_5 u(p)\mathcal{R}^B(s,t)\,, \tag{18}$$

where the $\sqrt{2}$ factor is understood in the meson sector in which vector, tensor, and axial mesons are written by the representative symbols for charged reactions. The mass parameter $m_0 = 1$ GeV and the t-channel momentum transfer $q' = q - k$, and momentum sum $P = \frac{1}{2}(p+p')$.

The tensor meson spin-2 projection is given by $\Pi^{\beta\rho;\lambda\sigma}(q') = \frac{1}{2}(\eta^{\beta\lambda}\eta^{\rho\sigma} + \eta^{\beta\sigma}\eta^{\rho\lambda}) - \frac{1}{3}\eta^{\beta\rho}\eta^{\lambda\sigma}$ with $\eta^{\mu\nu} = -g^{\mu\nu} + \frac{q'^\mu q'^\nu}{m_T^2}$.

The Regge propagator for an exchanged meson is written collectively for $\varphi(= V,\, T,\, A\, B)$,

$$\mathcal{R}^\varphi(s,t) = \frac{\pi\alpha'_\varphi \times \text{phase}}{\Gamma(\alpha_\varphi(\mathrm{t}) + 1 - \mathrm{J})\,\sin(\pi\alpha_\varphi(\mathrm{t}))}\left(\frac{s}{s_0}\right)^{\alpha_\varphi(s)-J}, \tag{19}$$

where the Regge phase $\frac{1}{2}((-1)^J + e^{-i\pi\alpha_\varphi(t)})$ in the canonical form is assigned to the spin-J meson for the exchange-nondegenerate case.

The Regge phase in production channels

The Regge phases for the electroproduction amplitudes from Eqs. (13) to (18) for charged reactions are chosen the same as in the case of photoproduction [**?**] which is expressed in schematic notation as follows,

$$\begin{aligned}\mathcal{M}(\gamma^* N \to \pi^\pm N) = \pm ie\pi\begin{Bmatrix} e^{-i\pi\alpha_\pi} \\ 1\end{Bmatrix} + b_1\begin{Bmatrix} e^{-i\pi\alpha_{b_1}} \\ -1\end{Bmatrix} \\ +\rho\begin{Bmatrix} -e^{-i\pi\alpha_\rho} \\ 1\end{Bmatrix} + a_2\begin{Bmatrix} -e^{-i\pi\alpha_{a_2}} \\ -1\end{Bmatrix} \\ \pm a_1\frac{1}{2}\left(-1 + e^{-i\pi\alpha_{a_1}}\right),\end{aligned} \tag{20}$$

where the $\sqrt{2}$ is omitted for brevity.

Gross-Riska prescription for nucleon and pion electromagnetic form factors

The nucleon charge form factor in the electromagnetic vertex given by

$$\Gamma_{\gamma^* NN}(k^2) = \widetilde{F}_1^N(k^2)\not{\epsilon} - \frac{\kappa_N}{4M}F_2^N(k^2)\,[\not{\epsilon},\not{k}] \qquad (21)$$

and pion charge form factor are chosen by following the Gross-Riska prescription

$$\widetilde{F}_1^N(k^2)\not{\epsilon} = F_1^N(k^2)\left(\not{\epsilon} - \not{k}\frac{\epsilon\cdot k}{k^2}\right) + F_1^N(0)\not{k}\frac{\epsilon\cdot k}{k^2}\,, \quad (22)$$

$$\widetilde{F}^\pi(k^2)(2q-k)\cdot\epsilon = F^\pi(k^2)(2q-k)\cdot\left(\epsilon - k\frac{\epsilon\cdot k}{k^2}\right) + F^\pi(0)(2q-k)\cdot k\frac{\epsilon\cdot k}{k^2}\,. \qquad (23)$$

B. The conventional Reggeized model

The proton electromagnetic form factors (EMFF) are considered in charged pion processes, which are expressed as

$$F_1^p(Q^2) = \frac{1+\tau\,\mu_p}{1+\tau}\left(1+Q^2/\Lambda_1^2\right)^{-2}, \qquad (24)$$

$$\kappa_p F_2^p(Q^2) = \frac{\mu_p - 1}{1+\tau}\left(1+Q^2/\Lambda_2^2\right)^{-2} \qquad (25)$$

with $\tau = Q^2/4M_P^2$ and $\Lambda_2 = \Lambda_1$.

In the description of the reaction cross sections model prediction with the magnetic term is worse than without it. Thus, it is usually neglected.

- In epion-tch-v2.exe, the cutoff Λ_1 is given as an input with the F_2 able to be turned on or off with cutoff $\Lambda_2 = \Lambda_1$ chosen automatically.

C. The Reggeized model with GPDs for proton EMFFs

For studying the partonic aspect of the reaction in the DIS regime, $Q^2 \ge 1$ GeV^2 and $W \ge 2$ GeV over the resonance region, we consider the case where the nucleon EMFF form factors parameterized by the GPDs in the $\gamma^* NN$ vertex which are written as,

$$F_1^p(Q^2) = \int_0^1 dx\,[e_u u_v(x) + e_d d_v(x)]\,x^{\alpha'_q(1-x)Q^2}, \quad (26)$$

$$F_1^n(Q^2) = \int_0^1 dx\,[e_d u_v(x) + e_u d_v(x)]\,x^{\alpha'_q(1-x)Q^2}, \quad (27)$$

$$F_2^p(Q^2) = \frac{1}{\kappa_p}\int_0^1 dx\left[\frac{e_u\kappa_u}{N_u}(1-x)^{\eta_u}u_v(x) + \frac{e_d\kappa_d}{N_d}(1-x)^{\eta_d}d_v(x)\right]x^{\alpha'_q(1-x)Q^2}, \quad (28)$$

$$F_2^n(Q^2) = \frac{1}{\kappa_n}\int_0^1 dx\left[\frac{e_d\kappa_u}{N_u}(1-x)^{\eta_u}u_v(x) + \frac{e_u\kappa_d}{N_d}(1-x)^{\eta_d}d_v(x)\right]x^{\alpha'_q(1-x)Q^2}. \quad (29)$$

Valence quark charge and anomalous magnetic momenta are $e_u = 2/3$, $e_d = -1/3$, $\kappa_u = 1.673$, and $\kappa_d = -2.033$, respectively. $\eta_u = 1.713$ and $\eta_d = 0.566$ from a fit to the nucleon form factor data. We make the slope parameter adjusted to obtain $\alpha' = 0.3$ which yields the same result from the $\Lambda_1^p = 1.55$ GeV.

The unpolarized valence quark densities are from Ref. Martin2002;

$$u_v(x) = 0.262x^{-0.69}(1-x)^{3.5}(1+3.83x^{0.5}+37.65x), \quad (30)$$

$$d_v(x) = 0.061x^{-0.65}(1-x)^{4.03}(1+49.05x^{0.5}+8.65x) \quad (31)$$

at the input scale $\mu^2 = 1$ GeV^2. For simplicity, the zero-skewness GPDs are implemented in the $\gamma^* NN$ vertex form factors throughout the work.

- In epion-tch-v2.exe, the slope α'_q is given as an input with the F_2 able to be turned on or off with the same slope α'_q chosen automatically.

In both approaches the monopole type of charge form factor is shared for the meson exchange in common,

$$F_\varphi(Q^2) = \left(1+Q^2/\Lambda_\varphi^2\right)^{-1} \qquad (32)$$

for $\varphi = \pi$, V, T, A, B and h_1,

In the Particle Data Group, it is reported that mesons of high spin are decaying to $a_1 \to \rho\pi$, $b_1 \to \omega\pi$, and $h_1 \to \rho\pi$, respectively. According to the Vector Meson Dominance, $a_1 \to \rho\pi \to \gamma\pi$, for instance, this leads to

$$\Lambda_{a_1} = 0.775 \text{ GeV}\,,\ \Lambda_{b_1} = 0.782 \text{ GeV}\,,\ \Lambda_{h_1} = 0.775 \text{ GeV}\,, \quad (33)$$

respectively. For the tensor meson a_2 exchange, we assume $\rho(1450) \to a_2\pi$ rather than the $\rho(775)$ and take the cutoff mass $\Lambda_{a_2} = 1.45$ GeV in order to assign its role similar to that in the case of photoproduction [**?**].

- In epion-tch-v2.exe, the cultoff Λ_π for pion exchange is given as an input with the cutoffs for

others fixed by the values given above.

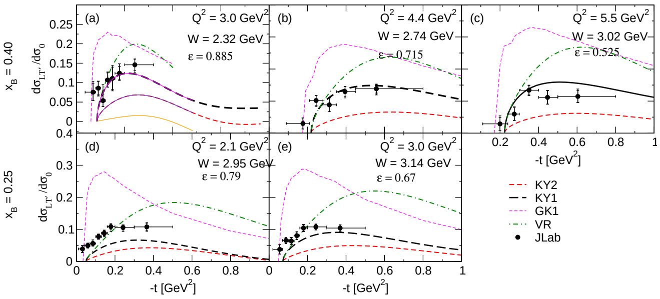

FIG. 1. t-dependence of $d\sigma_{LT'}/d\sigma_U$ for the exclusive reaction $p(e,e'\pi^+)n$ from JLab. **In epion-tch-v2, we choose the GPDs for F_1 and F_2 with α_q'=0.3 GeV^{-2} with Λ_π=775 MeV. a_1 with the sign positive is shown. In case of choosing dipole FF for F_1 and F_2, $\Lambda_1 = \Lambda_2$ =1.55 GeV with the same cutoff Λ_π.**

The role of the axial meson $a_1(1260)$ affects the SSA as well as the ratio of the cross sections $d(\pi^-p)/d(\pi^+n)$, so that the change of its sign leads to the different results. We once predicted the SSA with the sign of the a_1 positive. But the case of a_1 with the sign negative results in the better description of the SSA and the cross section ratio as well.

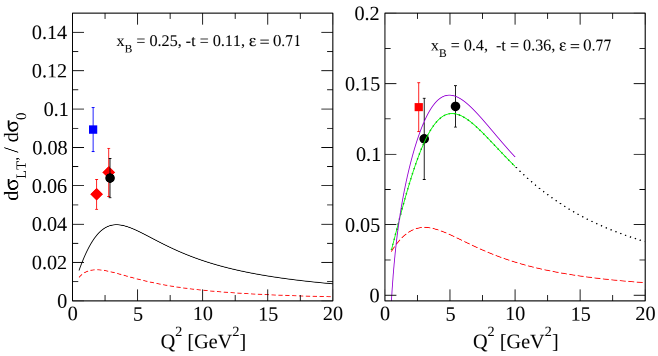

FIG. 2. Q^2-dependence of $d\sigma_{LT'}/d\sigma_U$ for the exclusive reaction $p(e,e'\pi^+)n$ from JLab. **In epion-tch-v2, we choose the GPDs for F_1 and F_2 with α_q'=0.3 GeV^{-2} with Λ_π=775 MeV. a_1 with the sign positive, or negative is shown.**

- In epion-tch-v2.exe, the sign of a_1 is given as an input to examine its effect on physical quantities.